

Preliminary Characterisation of Fast Time-of-flight Cameras for Optical Surface Tracking in Advanced Radiotherapy

S Y Lim and Hafiz M Zin

*Advanced Medical and Dental Institute, University Sains Malaysia,
Bertam 13200 Kepala Batas, Pulau Pinang Malaysia*

(Received: 2.2.2018 ; Published: 7.7.2018)

Abstract. Fast time-of-flight camera is an optical 3D imaging sensor that provides the depth information of a scene at a high frame rate. The technology is useful in advanced radiotherapy treatment that requires real-time patient setup information during the conformal dose delivery. The objective of this study is to characterise two CMOS-based commercial ToF cameras of different pixel array size, frame rate and light source for application in radiotherapy. The paper focuses on warm-up time test, dark current test, temporal noise test and background illumination test of Argos P320 and P330 ToF cameras (Bluetechnix, Austria). The characterisation tests were performed for each camera and the results obtained were analysed using MatLab. Overall, both cameras have a low temporal noise of 0.22% and submillimetre distance measurement accuracy. The results provide the performance characteristics of the sensor and the factors that influence the depth measurement accuracy. Future work will focus on the characterisation of the ToF camera in tracking object motion.

Keywords: time-of-flight camera; temporal noise; warm-up time; dark current

I. INTRODUCTION

With the advancement in technology, radiotherapy treatment technique has evolved from conventional 3D conformal radiotherapy treatment to intensity modulated radiation therapy (IMRT) and stereotactic body radiation therapy (SBRT), which utilise higher radiation dose and more conformal beam to improve treatment outcome [1]. The treatment margins become tighter and there is a greater potential for target miss due to patient setup variation and organ motion [2]. Hence, setup verification gains more importance compared to the conventional technique to ensure the accuracy of the treatment delivery.

Patient setup variation is the major source of uncertainty in radiotherapy [3]. Given that treatment is delivered over a number of fractions, it is important to ensure the accuracy of the patient positioning setup in each fraction. KV cone-beam computed tomography (CBCT) system and MV electronic portal imaging device (EPID) are the commonly used patient positioning verification system. The modalities provide volumetric or planar images to verify patient setup based on internal structures and allow immediate position correction prior to treatment [4,5]. However, the modalities have a limitation in tracking patient breathing motion in real-time. Furthermore, the patient is exposed to additional radiation dose, which can become substantial in

respect of the number of treatment fractions [6]. Hence, there is a need for a non-invasive image-based device that can verify and monitor patient motion during treatment.

Fast time-of-flight (ToF) camera is an emerging optical 3D imaging sensor that provides the depth information of a scene at the high frame rate. It consists of an illumination unit, which actively emits a high frequency modulated light signal to a target and a ToF sensor that detects the reflected light signals. The distance between the target and the camera is derived from the phase shift between the emitted and reflected light signals [7]. The application of ToF camera in gesture recognition, distance measurement and object tracking, is now widely used in the gaming, automotive and robotics industry [8].

ToF technology is useful in advanced radiotherapy treatment that requires real-time patient setup information to ensure accurate radiation dose delivery. Several studies on the feasibility of ToF technology for patient positioning and breathing motion gating have been performed [9,10]. ToF cameras are employed commercially in various industries but the measurement accuracy is affected by the imaging setting and environment condition. Characterisation of several other ToF cameras, like PMD CamCube 3.0, Mesa Swiss Ranger Cameras and Microsoft Kinect have been presented [11–14]. The objective of this study is to evaluate the noise and the depth measurement accuracy of two commercial ToF cameras: Argos^{3D} P320 (low image resolution sensor with LED illumination source) and Argos^{3D} P330 (high image resolution sensor with laser diode illumination source) for application in radiotherapy. Both cameras consist of an array of demodulation pixels, that can estimate the object depth based on the phase shift between the emitter and reflected light signal. Further details of the principles are described elsewhere [7].

II. MATERIALS AND METHODS

Description of Argos^{3D} P320 and P330 ToF camera

Two CMOS-based ToF cameras, Argos^{3D} P320 and P330 ToF cameras (Bluetechnix, Austria), as shown in Figure 1, are evaluated in this study. The TOF sensor used in Argos^{3D} P320 and P330 ToF cameras are CMOS-based Photonic Mixer Device (PMD) sensors manufactured by PMD Technologies (Siegen, Germany). The main specification of both ToF cameras is tabulated in Table 1. P320 and P330 are used to denote the ToF cameras in the remainder of this work. The P320 camera consists of a low-resolution ToF sensor with a pixel array of 160×120 pixels (PhotonICs@19kS3, PMD Technologies), incorporated with a near infra-red (NIR) LED illumination unit. Whereas, P330 camera consists of a higher pixel array of 352×287 pixels (TIM-U-IRS1020, PMD Technologies) and a high energy laser diode. The maximum accessible frame rate for both P320 and P330 ToF cameras are 160 fps and 28 fps, respectively. In this work, the performance of both ToF cameras at higher frame rate is studied. The ToF cameras generate two different images synchronously: distance image, which is based on the phase-shift estimation and amplitude image, which is computed based on the strength of the reflected light signal.

TABLE 1. The specification of the evaluated ToF cameras.

Camera Model	P320	P330
Array size	160 × 120	352 × 287
Modulation frequency	5-30 MHz	5-100 MHz
Frame rate	10-160 fps	10-28 fps
Field of view (FoV)	90°	110°
Type of illumination unit	High power LED	High power laser diode

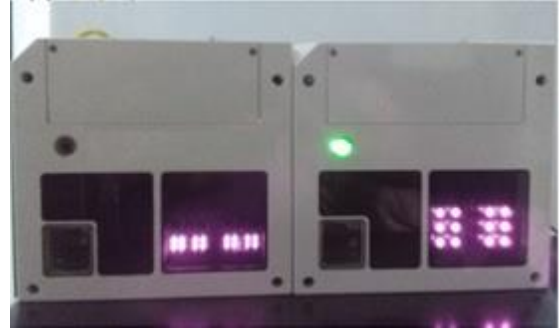


FIGURE 1. P320 (right) and P330 (left) camera

Experiment Description

The evaluation of both P320 and P330 camera were performed in a dark room. In all experiments, ToF camera was placed at the edge of a table, facing towards a lab wall that was covered with a blackout curtain. A white planar target of dimension 50 cm × 72 cm was placed in front of the camera at a distance of 100 cm (as shown in Figure 2). The dimension of the target and the distance chosen are based on the opening angle and the imaging setting of the camera such that two-thirds of the FoV is covered by the target. The camera setting of each experiment is listed in Table 2 and all the available internal filters were deactivated before the experiment.

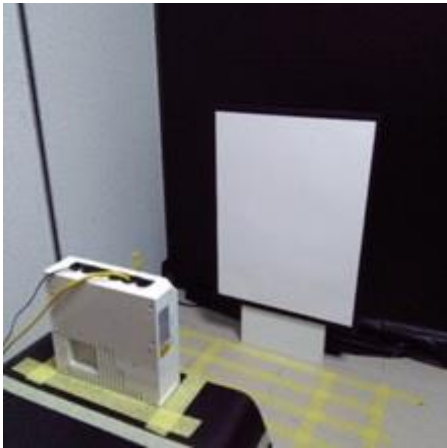


FIGURE 1. The camera setup for warm-up time test.

TABLE 2. The camera settings used in each experiment.

Model	Modulation Frequency (MHz)	Frame rate (fps)	Integration Time (ms)
P320	20	10	0.70
		80	0.35
	30	10	0.90
P330	20	80	0.51
		10	1.04
	30	28	0.98
		10	1.00
		28	0.45

Warm-up Time Evaluation

The ToF cameras are fabricated in standard CMOS technology and the increase in circuit density may resulted in thermal issues due to higher power consumption [15]. Both ToF cameras were operated at room temperature without additional sensor cooling system. Throughout the image acquisition process, the temperature of the sensor may increase and the illumination light may transfer thermal energy to the sensor. The increase in temperature changes the response of the camera and lead to a drift in distance measurement [16]. The distance drift becomes constant as the sensor temperature achieves thermal equilibrium. In order to quantify the time needed for the ToF camera to reach the thermal equilibrium state, a warm-up time evaluation was performed. In this experiment, the white planar target was placed at 100 cm in front of the ToF

camera. The integration time of P320 and P330 camera was set to 1000 μs and 1750 μs , respectively. A region of interest of 9×9 pixels at the centre of the distance image was selected and the distance data was captured continuously for 120 minutes. The distance data was saved in .csv format and evaluated using MatLab (The MathWorks, Natick, MA). The distance data was averaged over one second to reduce the influence of temporal noise. The distance measured in the last ten minutes was averaged and referred to as the steady state of the camera. Distance drift is derived by normalising the averaged distance data with the average distance value during the steady-state. A distance drift over time of both ToF cameras was plotted.

Dark Current Evaluation

Dark current is defined as the rate of the heat-induced electron released from the semiconductor chip without light exposure. The aim of this experiment is to quantify the inherent dark current of the ToF camera. In this experiment, the ToF camera and the illumination unit were covered with blackout materials. A region of interest of 9×9 pixels at the centre of the amplitude image was selected. After warming up the ToF camera, 100 consecutive frames are captured for different integration times. Dark signal against integration time of each ToF cameras was plotted and the gradient of each plot was calculated.

Background Illumination Influence

ToF camera estimates the distance of a target object based on the amount of the reflected light signals. The environment or background illumination may impact the accuracy of the distance measurement. The objective of the experiment is to evaluate the distance variation due to the background illumination influence. The camera setup is similar to that as proposed by Fürsattel *et al.* [14], where the distance between the ToF camera and the target is 80 cm and the size of the ROI selected is 9×9 pixel. The camera setting was listed in Table 2. With the same selection of ROI, 100 consecutive frames are captured with room lights were on and off. The mean distance, \bar{x} , and the standard deviation, σ , of the 100 frames taken were calculated.

Temporal noise Evaluation

Temporal noise is the variation of distance measurement over time. The variation is more evident with low illumination light source or low reflectivity target object. In this experiment, the influence of target reflectivity on the measurement noise is determined. The setup of the ToF camera was the same as in the background illumination test and 100 consecutive frames were taken. The experiment was repeated with a black paper foreground. The mean distance, \bar{x} , and the standard deviation, σ , of the 100 frames taken were calculated. The temporal noise was calculated by dividing the standard deviation of the 100 frames over the mean distance value

III. RESULTS AND DISCUSSION

Figure 3(a) and (b) displayed the warm-up results of both P320 and P330 ToF cameras. During the warm-up test, the sensor temperature of P320 and P330 camera increased gradually from 28°C to 37°C and 20°C to 30°C , respectively. For P320 camera, the distance drift increased gradually in the first 41 minutes and reached thermal equilibrium. Whereas, for P330 camera, the warm-up time needed is 24 minutes. Besides, distance drift variation of P330 camera is within 2

mm, compared to 4 mm in P320 camera. This is because of the application of laser diode as the illuminator, which produces a more coherent light signal. Hence there is less scattered light signal and in turn, resulted in lower image noise in P330 camera.

The dark current results of both P320 and P330 ToF camera are shown in Figure 4. For P320 camera, the dark signal increases linearly over the range of integration time and the dark current generated is 0.324 DN/ms. While for P330 ToF camera, the dark signal increases in a small magnitude of 0.11 on average as the integration time increased and the range of the dark signal obtained is within 5 – 6 DN. The dark current generated is 0.034 DN/ms, which is approximately ten times lower than that of P320 camera. Overall, the dark current noise inherent in both ToF camera is relatively low compared to other noise error. This may due to the fabrication of the CMOS sensor, which involved the utilisation of pinned photodiode technology or the application of a thinner dielectric stack, which reduce the generation of dark current [18].

Table 3 displays the distance measurement obtained when the room light is on and off. The distance variation for both sensors is within 1 mm, even though the distance data is acquired at a higher frame rate. Besides, the discrepancy of the distance measurement of both ToF cameras due to the background illumination is less than 0.22%. The sensor is less affected by the external lights because of the use of the narrow bandpass optical filter, which only allows the light signal with a wavelength of 850 nm to reach the sensor [19]. Furthermore, the pixel circuitry will further suppress the background illumination by integrating the reflected signals of 0°, 90°, 180° and 270° phases into two different bins alternately, on which the difference of the bin is used to determine the signal amplitude. Equal charges are added to both bins simultaneously to prevent saturation effect. This will, in turn, reduce the background illumination effect, resulting in an increase in the signal-to-noise ratio (SNR) and dynamic range of the demodulation pixel [19,20].

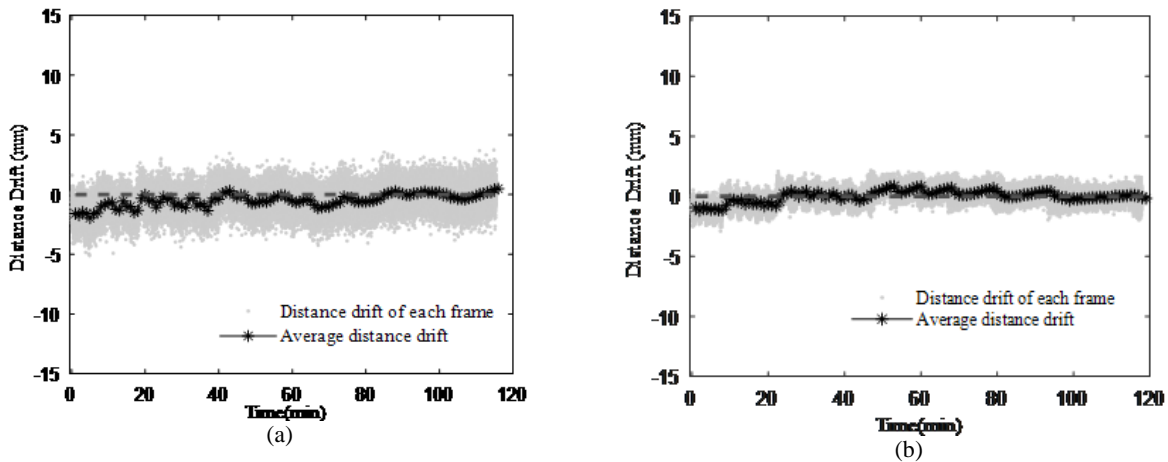


FIGURE 2. Distance drift over 120 minutes for (a) Argos^{3D} P320 and (b) Argos^{3D} P330. The grey dot represents the average of 9×9 ROI each frame captured and the black line is referred to the average distance drift per second.

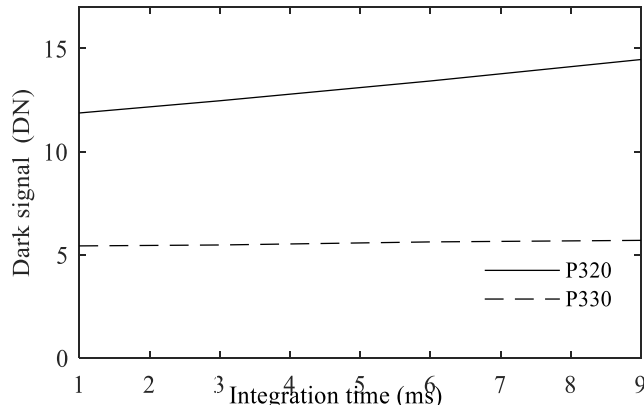


FIGURE 3. Dark signal against integration time plot of Argos^{3D} P320 and Argos^{3D} P330 ToF camera.

TABLE 3. The distance measurement obtained in dark room and with lights on for both P320 and P330 camera.

Model	Modulation Frequency (MHz)	Frame Rate (fps)	Distance Measurement, \bar{x} (mm)		Discrepancy of Distance measurement (mm)	Influence of Background Illumination (%)
			Lights off	Lights on		
P320	20	10	800.33	802.06	0.33	-0.22
		80	799.72	799.71	-0.28	0.00
	30	10	799.89	800.77	-0.11	-0.11
		80	800.60	799.71	0.60	0.11
P330	20	10	800.93	800.74	0.93	0.02
		28	800.26	800.22	0.26	0.00
	30	10	799.55	799.79	0.45	-0.03
		28	800.87	801.00	0.87	-0.02

The temporal noise evaluation results are shown in Table 4. The temporal noise of the distance of the white planar target are within 0.22% and 0.09% for P320 and P330 ToF cameras respectively. For the black planar target, the temporal noise and standard deviation of P320 ToF camera are doubled and the distance measured decreased by 10 - 40 mm compared to the white target. The temporal noise characteristic of P320 is consistent with that of Argos P100 (Bluetechnix, Austria) and PMD CamBoard nano (PMD Technologies, Siegen, Germany) in Fürsattel *et al.* work [14], in which the ToF sensors are the same. The changes in terms of the distance measured and the standard deviation is due to less light signals are reflected by the low reflectivity black target. For both cameras, the effect of the low reflectivity target was shown in the changes of the distance measured; however, the temporal noise acquired with both white and black planar targets are the same for P330. This is because of the application of the laser illuminator in P330 ToF camera, which generates more coherent and less scattered light signals and hence the yielded temporal noise is the same although the amount of reflected light signals from both white and black planar target are different.

TABLE 4. The temporal noise results obtained for both P320 and P330 camera.

Model	Modulation Frequency (MHz)	Frame Rate (fps)	White		Black	
			Distance measurement (mm)	Noise (%)	Distance measurement (mm)	Noise (%)
			$[\bar{x} \pm \sigma]$		$[\bar{x} \pm \sigma]$	
P320	20	10	800.33 \pm 0.60	0.07	761.88 \pm 1.11	0.15
		80	799.72 \pm 1.76	0.22	769.45 \pm 3.80	0.49
	30	10	800.64 \pm 0.44	0.05	774.83 \pm 0.68	0.09
		80	800.60 \pm 1.03	0.13	775.19 \pm 2.25	0.29
P330	20	10	800.93 \pm 0.46	0.06	832.57 \pm 0.44	0.05
		28	800.26 \pm 0.70	0.09	812.33 \pm 0.72	0.09
	30	10	799.55 \pm 0.38	0.05	779.36 \pm 0.33	0.04
		28	800.87 \pm 0.54	0.07	769.51 \pm 0.78	0.10

IV. CONCLUSION

In this paper, the performance characteristics of both P320 and P330 ToF cameras have been studied. Overall, both ToF cameras have a submillimetre distance measurement accuracy of a static object. The background illumination has little effect on the measurement accuracy. P330 ToF camera has a lower temporal and dark current noise compared to P320. Besides, the warm-up time for P330 ToF camera is 17 minutes shorter than P320 ToF camera. This is due to the higher pixel array size and the laser light source used in the ToF camera. Future work will focus on the characterisation of ToF camera in tracking object motion.

ACKNOWLEDGEMENTS

This work was funded by Fundamental Research Grant Scheme (FRGS), Ministry of Education Malaysia, with the project code of 203/CIPPT/6771383.

REFERENCES

1. J. Thariat, J.M. Hannoun-Levi, A. Sun Myint, T. Vuong, and J.P. Gérard, “Past, present, and future of radiotherapy for the benefit of patients.”, *Nat. Rev. Clin. Oncol.* **10**, 52-60 (2012).
2. R. Baskar, K. A. Lee, R. Yeo, and K.W. Yeoh, “Cancer and Radiation Therapy: Current Advances and Future Directions.”, *Int. J. Med. Sci.* **9**, 193-199 (2012).
3. B. Barbes, J. D. Azcona, E. Prieto, J. M. de Foronda, M. Garcia, and J. Burguete, “Development and clinical evaluation of a simple optical method to detect and measure patient external motion.”, *J. Appl. Clin. Med. Phys.* **16**, 306-321 (2015).
4. J. Boda-Heggemann, F. Lohr, F. Wenz, M. Flentje, and M. Guckenberger, “kV cone-beam CT-based IGRT.”, *Strahlentherapie Und Onkol.* **187**, 284-291 (2011).
5. J. Garayoa and P. Castro, “A study on image quality provided by a kilovoltage cone-beam computed tomography.”, *J. Appl. Clin. Med. Phys.* **14**, 239-257 (2013).
6. M. Gilles, H. Fayad, P. Migliorini, J. F. Clement, S. Scheib, L. Cozzi, J. Bert, N. Bousson, U. Schick, and D. Visvikis, “Patient positioning in radiotherapy based on surface imaging using

- time of flight cameras.”, *Med. Phys.* **4833**, 4833-4842 (2016).
7. R. Lange and P. Seitz, “Solid-state time-of-flight range camera.”, *IEEE J. Quantum Electron.* **37**, 390-397 (2001).
 8. S. L. X. Francis, S. G. Anavatti, M. Garratt, H. Shim, “A ToF-Camera as a 3D Vision Sensor for Autonomous Mobile Robotics.” *Int. J. of Adv. Robot Syst.* **12** (2015).
 9. C. Schaller, Time-of-Flight - A New Modality for Radiotherapy., 1-125 (2011)
 10. S. Placht, J. Stancanello, C. Schaller, M. Balda, E. Angelopoulou, “Fast time-of-flight camera based surface registration for radiotherapy patient positioning.” *Med Phys* **39**, 4-17 (2011)
 11. S. Foix and G. Aleny, “Lock-in Time-of-Flight (ToF) Cameras : A Survey.”, *IEEE Sens. J.* **11**, 1-11 (2011).
 12. L. Yang, L. Zhang, H. Dong, A. Alelaiwi, and A. El Saddik, “Evaluating and improving the depth accuracy of Kinect for Windows v2.”, *IEEE Sens. J.* **15**, 4275-4285 (2015).
 13. D. Piatti and F. Rinaudo, “SR-4000 and CamCube3.0 Time of Flight (ToF) cameras: Tests and comparison.”, *Remote Sens.* **4**, 1069-1089 (2012).
 14. P. Fürsattel, S. Placht, M. Balda, C. Schaller, H. Hofmann, A. Maier, and C. Riess, “A Comparative Error Analysis of Current Time-of-Flight Sensors.”, *IEEE Trans. Comput. Imaging* **2**, 27-41 (2016).
 15. F. Chiabrando, R. Chiabrando, D. Piatti, and F. Rinaudo, “Sensors for 3D imaging: Metric evaluation and calibration of a CCD/CMOS time-of-flight camera.”, *Sensors* **9**, 10080-10096 (2009).
 16. H. Handel, “Analyzing the influences of camera warm-up effects on image acquisition.”, *IPSI Transactions On Computer Vision And Application.* **1**, 258-268 (2009).
 17. J.P. Carrere, S. Place, J.P. Oddou, D. Benoit, and F. Roy, “CMOS image sensor: Process impact on dark current”, IEEE International Reliability Physics Symposium Proceedings. (2014).
 18. M. Heredia Conde, “Phase-Shift-based Time-of-Flight Imaging System,” in *Compressive Sensing for the Photonic Mixer Device*, Wiesbaden: Springer Vieweg, 2017, pp. 11-79.
 19. C. Hertzberg and U. Frese, “Detailed Modeling and Calibration of Time-of-flight Camera”, Proceedings 11th International Conference Informatics Control Automation Robotic, 2014, pp. 568-579.